ISSN: 2229-7359 Vol. 11 No. 3,2025

https://theaspd.com/index.php

# Smart Monitoring of Urban Heat Islands in Algiers, Algeria: A Hybrid Approach Using Mobile Sensors and Satellite Data

Maamar Ayouaz<sup>1</sup>, Abderrahmane Medjerab<sup>2</sup>, Nabil Mega<sup>3</sup>

<sup>1,2</sup>F.S.T.G.A.T, USTHB - Box.P.32, El Alia, Bab Ezzouar, 16111, Algiers/ Algeria <sup>3</sup>Hamma Lakhdar University, P.O. Box: 789, El Oued/ Algeria. ayouaz@geosmatic.dz<sup>1</sup>, a.medjerab@gmail.com<sup>2</sup>, mega-nabil@univ-eloued.dz<sup>3</sup>

### Abstract

Due to fast urbanization, urban heat islands (UHIs) raise urban temperatures and have been widely studied/monitored for their implications on quality of life, public health, and energy use under climate change. This article introduces a smart monitoring approach from studying the UHIs in Algiers, Algeria, a densely populated Mediterranean city sensitive to extreme heat events like the heat wave of July 2019. Two vehicle-mounted prototypes measuring air temperature and humidity were deployed to collect data, complemented by three satellite images for land surface temperature (LST) analysis and mapping. Data processing included matching mobile measurements with satellite overpasses, computing land surface temperature (LST) using a standard algorithm, and mapping urban heat islands (UHIs) with the help of geographic information systems (GIS) interpolation. The results demonstrated an important linear relationship between sensor air temperature and LST in Algiers (R2 = 0.752), where discrepancies between sensor air temperature and LST revealed the complexities of the UHI phenomenon. The study proves that smart monitoring is possible, but also shows that the methods must be improved in order to provide accurate and scalable monitoring. It set the stage for dynamic visualization on a web server, which facilitated realtime heat wave alerts. However, constraints of limited sensor coverage underuse of humidity data, and vehicle-related biases limit the scalability of this approach. This approach enhances urban heat island (UHI) characterization over conventional approaches, providing a flexible platform for climate adaptation initiatives in cities, one that can be extended beyond UHI following optimization.

Keywords: Algiers, Urban Heat Islands, Smart Monitoring, Landsat 8, GIS.

### INTRODUCTION

Urban heat islands (UHIs) are an important environmental issue that introduces area temperatures much higher than their surrounding rural counterparts in metropolitan areas because of the degree of urbanization and modified land surface properties (Oke, 2002). This phenomenon stems from the rising residential density, expansion of impermeable surfaces like pavements and buildings, as well as loss of vegetation which reduces evapotranspiration and increases solar radiation absorption (Arnfield, 2003; Stewart & Oke, 2012). Under global climate change, UHIs exacerbate heat waves and affect urban life quality, health, and energy consumption (Heaviside et al., 2017; Santamouris, 2015). A recent study, for example, estimates that 17,000 UHI-related deaths occur yearly across 93 cities in Europe, or approximately 6,700 premature deaths per city per year, representing 4% of summer mortality (Masselot et al., 2023). The observation and estimation of UHIs have received growing attention from global research. Common methods tend to utilize satellite images (Landsat data, for example), in order to evaluate land surface temperature (LST) levels and map thermal dispersion (Weng et al., 2004; Voogt & Oke, 2003). Gémes et al. (2016) utilized this technique in Vancouver, Canada, but established a poor correspondence (R2 = 0.38) between LST and ambient air temperature exposing the limitations of satellite data in adequately capturing real-time thermal dynamics.

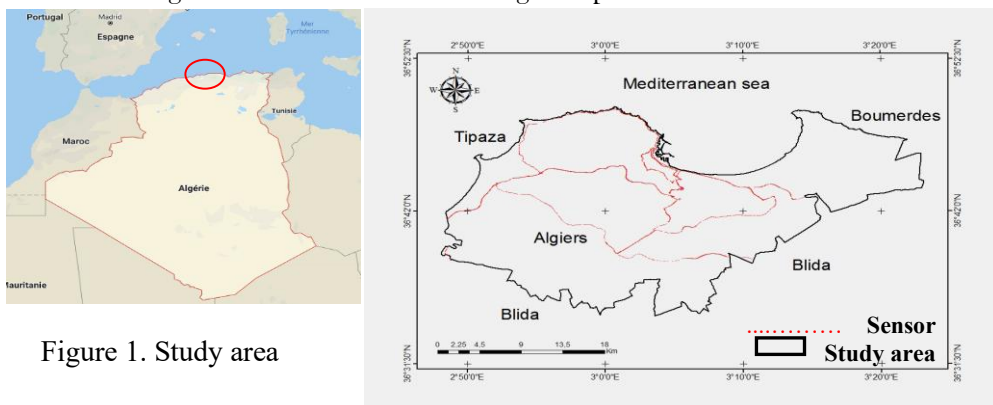
ISSN: 2229-7359 Vol. 11 No. 3,2025

https://theaspd.com/index.php

Yasuyo Şahin et al, Doha, Qatar. (2011) used statistical models (OLS, RTA, RF) and Landsat imagery, finding complex thermal gradients but poor spatial resolution (restrictive at the local scale). In contrast, Chotchaiwong et al. In India (2019), also noted strong collinearity between LST and air temperature (R2 = 0.446 in January, R2 = 0.658 in April), validating satellite utility for partial temporal application exposure. UHI research is scarce in Algeria even as the country has extreme climatic conditions, especially in the desert and urban areas. Boukhebla et al. (2013) and Amieur et al. The role of the local architecture in UHI mitigation was examined in Biskra and Ghardaïa by working on the impacts of traditional architectural practices of traditional architecture (2022), showing the effectiveness of local materials and vegetative belts. Yet, in large cities such as Algiers - where the density of population is estimated to be 8231.80 inhabitants per km2 (ONS, 2008) and heat waves are escalating, evidenced by an anomaly of +3.3°C over the monthly average temperatures in July 2019 (ONM, 2019) - classical techniques developed based on low numbers of weather stations (distributed between 5 and 15 km) or imagery from satellite (acquired every 16 days at 11:30 local time) are not able to accurately observe the UHIs whose thermal peaks usually appear between 12:00 and 15:00 (Akbari et al., 2001). These are developments which recent study urges enormous pressure to come up with solutions. Zhao et al. (2014) showed that UHIs were more intense in humid climate, whereas Marando et al. (2021), project their escalation until 2030 due to urban sprawl and lack of green infrastructure. Moreover, the interaction between UHIs and heat waves increases health risks, especially for sensitive populations (Li et al., 2019). Yao et al. in the work of Wang et al. (2021), a significant increase in the intensity of the UHI phenomenon was recorded between 1990 and 2010 and related to increases in impervious surfaces. To tackle these challenges, this research presents a smart monitoring approach for UHIs in Algiers by combining mobile temperature and humidity sensors (mounted on vehicles) with Landsat 8 data. This approach intends to address the spatiotemporal constraints associated with current methodologies and provide dynamic UHI mapping as derived from ultra-high efficiency environmental sensors and MRS (Ramírez et al., 2021; Xian, 2023).

#### Study area

The study area is in the city of Algiers in northern Algeria (Fig. 1), bordered by the Mediterranean Sea to the north, the Boumerdès Province to the east, the Blida Province to the south and the Tipaza Province to the west (Fig. 1). Based on the 2018 statistics from the Office National des Statistiques (ONS), Algiers has a population of 2,988,145 inhabitants, with a density of 8,231.80 inhabitants per kilometer<sup>2</sup>. With the Mediterranean climate, the city has witnessed record heatwave episodes. In particular, July 2019 was so hot, both daytime and night, that heat records were broken in several parts of the country. In the meantime, the national climatological center of the office national de la météo (ONM), has indicated that the average temperature in excess of the climatological norm at +3.3 °c during this period.



ISSN: 2229-7359 Vol. 11 No. 3,2025

https://theaspd.com/index.php

#### DATA AND MATERIALS

The study involves an analysis of a UHI in Algiers, Algeria, combining meteorological data, satellite information, and a specially designed electronic prototype. The main data sources consisted of daily time series of air temperature and humidity, obtained from thirteen weather stations (Office National de la Météorologie (ONM)), which were located throughout the entire study area. These in-situ measurements served as a reference for validating both the spatial and temporal information related to temperature and humidity in the city. Three satellite images were utilized in conjunction with the in-situ data. Land surface temperature (LST) with 30 m spatial resolution was derived from two Landsat 8 images (22 and 23 July 2022). The surface thermal patterns were derived from these images to identify the UHI areas. UHI distributions were visualized in the context of high resolution Quickbird image (0.50 cm spatial resolution) as cartographic base of the same region. An important part of this research involved developing a mobile electronic prototype for real-time measurement of air temperature and humidity. The following components made up the prototype:

A microcontroller (Lopy, ESP32 model) made by Pycom with Wi-Fi and Bluetooth functionalities for data transmission.

Factory calibrated Digital Temperature & Humidity Sensor from Sensirion.

An external power source such as a power bank or 3 1.5 V batteries that provides a regulated voltage supply of 4.5 to 5 V to enable continuous operation.

A motherboard with an integrated SD card reader that wrote down the temperature, humidity, time, and geographic position data in a comma separated values (CSV) file.

A GPS module attached to the microcontroller to generate UTC time and precise geolocation coordinates for each measurement.

These elements were then packaged into a small, portable unit (Fig. 2), deploying on vehicles for data collection in a dynamic context covering the entirety of Algiers. The inclusion of GPS functionality provided spatial referencing of the measurements, directly comparable to the satellite based LST data. This novel prototype has potential to address limitations of traditional fixed weather stations and periodic satellite imagery due to their ability to provide a higher temporal resolution and flexibility in obtaining observations of UHI dynamics.

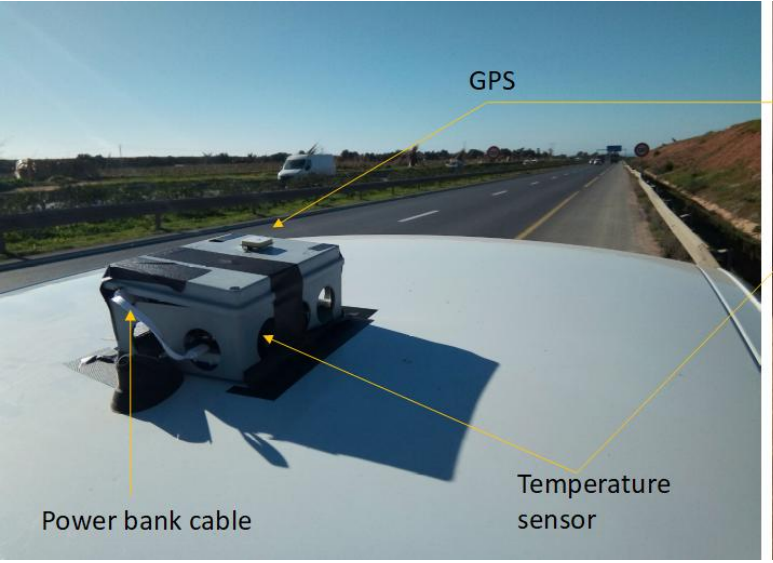




Figure 2. Design of the mobile temperature sensor

ISSN: 2229-7359 Vol. 11 No. 3,2025

https://theaspd.com/index.php

#### METHODOLOGY

To overcome some limitations of the conventional UHI monitoring methods, the methodology adopted in this study involves high-resolutions, real-time data collection integrated with satellite-based observations. This hybrid approach was created to improve the quality of temperature and humidity measurement in terms of spatial/temporal resolution throughout Algiers, Algeria, allowing the total UHI analysis. We deployed mobile sensors to acquire data timed with satellite overpasses before calculating land surface temperature (LST) from satellite imagery followed by spatial mapping of UHI zones through four main steps. They are described step-wise as this provides a clear framework for the processes of data collection and analysis.

# Deployment of mobile sensors

Two identical prototypes were assembled and mounted on separate vehicles to collect in-situ measurements of air temperature and humidity, as described in Section 3. Based on mobile meteorological observation protocol (e.g. Cao et al., 2023), the sensors were placed to avoid interference from heat sources (such as engine and exhaust system) and the high number of sensors that could affect the detour of traffic vehicles. Before deployment, the sensors were checked against a reference thermometer before deployment to ensure they operated within ±0.2 °C accuracy as specified by Sensirion, the sensor manufacturer. To capture spatial variability of UHI intensity, the vehicles were driven along a priori defined paths over a range of urban morphology in Algiers from dense built atmosphere, coastal and peri-urban landscapes.

# Data-synchronization and acquisition

Data collection was scheduled to coincide with the overpass of the Landsat 8 satellite, which crosses the study area every 16 days around 11:30 local time (UTC +1). To cover the diurnal evolution of Urban Heat Islands (UHIs) as much as possible, recordings were taken continuously from one hour prior to the satellite overpass (10:30 local time) up to 16:00 local time, with additional nocturnal sampling for some days to check the nighttime UHI effects. The speed of the data logging was set to 5 seconds, and the parameters stored were air temperature, relative humidity, UTC time, and GPS coordinates (latitude and longitude), which were written as CSV file format to the SD card. Simultaneously, measurements were made next to the 13 ONM weather stations to allow cross-checking with fixed meteorological data. This temporal and spatial synchronization allowed for a direct comparison of mobile-obtained LST between both satellite-derived and ground-truth LST data.

# Calculation of land surface temperature (LST)

We obtained LST from Landsat 8 images on 2018-01-17 and 2015-07-04 using a single channel algorithm (Jiménez-Muñoz et al., 2014). An overview of the steps is provided below:

Satellite image and data preparation (1) Radiometric Correction: The Landsat 8 thermal infrared band (Band 10) was converted from digital numbers (DN) to top-of-atmosphere radiance according to the calibration coefficients provided by the United States Geological Survey (USGS); Atmosheric Correction: Subsequently the atmospheric effects were corrected using the radiative transfer equation combined with inputs of water vapor content and atmospheric profiles retrieved from the MODIS Atmospheric Profile product (MOD07) over the respective dates.

Emissivity estimation: Earth surface emissivity was estimated based on Landsat 8 normal difference vegetation index (NDVI) derived from visible and near-infrared from Landsat 8 visible at Band4 and Band5 following the Sobrino et al. (2004). Land cover types (e.g., urban surfaces, vegetation) were used to inform emissivity values.

LST Retrieval: The radiance with the previous correction was transformed to surface temperature via the Planck function, considering emissivity and the considered atmospheric parameters.

ISSN: 2229-7359 Vol. 11 No. 3,2025

https://theaspd.com/index.php

The resulting 30-meter resolution LST maps offered a continuous spatial baseline to characterize UHI zones in Algiers at the times of the satellite overpass.

# Mapping temperature

In order to evaluate the differences between the air temperature (from mobile sensors) and LST (from Landsat 8), a temperature difference analysis was performed. For each measurement point logged by the mobile sensors, the respective LST value extracted (via the GPS coordinates using the satellite-derived raster as a spatial reference) Differences were calculated as (Eq. 1):

 $\Delta T$  = Tsensor — TLandsat

(Equation 1)

Where Tsensor: air temperature measured by the mobile prototype.

TLandsat: LST at the same point.

Statistical analyses focused on determining correlation coefficients and recognizing patterns related to urban morphology, vegetation cover, and distances from the coast. Finally, the integrated dataset (including mobile sensor measurements, Landsat LST and Quickbird imagery) was computed using a geographic information systems (GIS) environment (ArcGIS 10.8). For UHI maps to create the temperature and humidity values (humidity data are not shown in this paper) across unobserved regions, we applied the inverse distance weighting method (IDW) for interpolation methods. One of the base maps used primarily for visualization by overlaying the UHI interpolated maps on it was a high resolution Quickbird image which helped to visualize the identified hotspots with respect to the other urban features (e.g. roads network and building density).

# Data management and validation

All data were transmitted in real-time to a dedicated web server (www. heatislands. net) through the prototypes' Wi-Fi capabilities, where they were saved in a time-series database. Temporal trends and spatial distributions were visualised using the open-source platform Grafana, enabling real-time monitoring and analysis. The mobile sensor measurements were validated against ONM station data using Pearson's correlation coefficient and root mean square error (RMSE) to evaluate data quality and providing a quantitative assessment of the prototype's reliability.

## **RESULTS AND DISCUSSION**

The 2 mobile prototypes were used to collect real-time temperature and humidity data across Algiers in synchronisation with the Landsat 8 overpass and the 13 weather stations operated by the Office National de la Météorologie (ONM), to compare with in situ measurements. In terms of summary, Table 1 (Table 1 extracted) shows the results of the extraction of 10:23:04 to 10:25:44 UTC (26 rows) which shows significant differences between air temperature from mobile sensors (TempSensor) and land surface temperature (LST) from Landsat 8 at the same time (Temp-Landsat). As an instance, at 10:23:04 UTC (PT967), the mobile sensor recorded 15.65°C and the relevant LST was 14.84°C, while at 10:24:04 UTC (PT978), the air temperature recorded 16.5°C and the LST was 14.56°C, with a total mean deviation of 0.15 to 1.94°C over the dataset. This difference, from 0.07°C (PT987) to 1.94°C (PT978), also corresponds with results from Voogt and Oke (2003) who suggest that explanations for similar differences can be ascribed to underestimation of air temperature within thick urban surroundings due to the radiative properties of urban surfaces. Similarly, Peng et al. (2000) in 1014 cities, and more recently 419 global cities documented similar disparity due to the low emissivity of concrete and other urban materials (2012). The mobile sensors also showed a capacity to identify micro-scale thermal gradients that were not visible in the static ONM network. On a 210 m transect between PT967 (494761.845, 4067002.587) and PT992 (494972.136, 4066961.417), sensor air

ISSN: 2229-7359 Vol. 11 No. 3,2025

https://theaspd.com/index.php

temperature decreased from 0.81 °C to 0.15 °C in 2 min 40 s (n = 4), a drop of 0.66 °C, indicating localized heat island effects which may be driven by the presence of concentrated impervious surfaces or reduced ventilation. The peak at PT978, 1.94°C, then a drop to 1.28°C 15 seconds later at PT980, illustrates the prototype's capability for detecting rapid spatial transitions, which is lost from the smoothing of fixed stations tens of km apart (Arnfield, 2003; Stewart & Oke, 2012). This capability echoes Cao et al. (2023), employed mobile sensors in Shanghai for small-scale UHI detection to improve urban thermal simulation models. Sensors have a high temporal resolution (5 s sampling) leading to a significant improvement over satellite imagery that provide a single snapshot at 11:30 local time while UHI peaks typically occur later in the day. A strong relationship (coefficient of determination, R2 = 0.752) was found between mobile sensor and Landsat 8 measurements through statistical analysis. This is even stronger than the R2 = 0.38 Gémes et al. (2016) and is sufficient with the values of Chotchaiwong et al. (2019), confirming the prototype's efficacy in honing in on satellite estimates. Yet, the dataset highlights peculiarities surrounding warmer states; at PT988 and PT989, where humidity peaked at 60% (compared to 50% otherwise), air temperatures plummeted to 13.70°C and 13.90°C (respectively), indicating a thouht froging effect not pe proceeding in this analysis but attested by Santamouris (2015). Wang et al. (2019) point out that humidity can also reduce perceived UHI intensity in coastal cities by up to 20%, highlighting the need to integrate this parameter in future work. Combining diverse data (mobile sensors and Quickbird/Landsat imagery) for the spatial mapping of UHIs in Algiers indicated heterogeneous heat distribution in the city, where densely built areas such as Bab El Oued were observed to be warmer than the peri-urban and coastal zones, a feature generally related to UHIs (Weng et al., 2004). The web server (www. heatislands. net) and Grafana with the potential for dynamic visualization, as well as possible real-time heatwave alerts (as shown in July 2019). This is consistent with the findings of Tzyrkalli et al. (2024), who emphasise the importance of real-time monitoring in linking UHI health impacts and countermeasures in the Global South, specifically in African cities. However, some limitations remain: two sensors create coverage gaps in remote locations (e.g., terrain, lakes) and the short temporal window in Table 1 (2 min 40 s) precludes along-track views. The monitoring of humidity data, although collected, has not been fully utilized (Ramírez et al., 2021), and there are biases associated with vehicles (Zhou et al. (2019) need more control to keep them scalable.

Table 1. Extracted table from sensors and Landsat data.

UTC	TempSensor	Humidity	X	Y	Temp-Landsat
10:23:04	15,65	50	494761,8	4067003	14,84
10:23:09	15,84	50	494769,5	4067001	14,81
10:23:14	15,98	50	494771,2	4067001	14,81
10:23:19	16,08	50	494772,5	4067000	14,8
10:23:24	16,27	50	494773,6	4067000	14,8
10:23:29	16,01	50	494777,7	4066999	14,78
10:23:34	15,72	50	494787,5	4066997	14,74
10:23:44	15,92	50	494800,5	4066995	14,66
10:23:49	15,99	50	494802,2	4066995	14,65
10:23:54	16,13	50	494802,9	4066995	14,64
10:23:59	16,34	50	494803	4066995	14,64
10:24:04	16,5	50	494802,9	4066995	14,56
10:24:14	15,89	50	494814,5	4066993	14,46
10:24:19	15,58	50	494825,6	4066990	14,3
10:24:29	15,04	50	494839,1	4066987	14,18
	10:23:04 10:23:09 10:23:14 10:23:19 10:23:24 10:23:29 10:23:34 10:23:49 10:23:54 10:23:59 10:24:04 10:24:19	10:23:04 15,65 10:23:09 15,84 10:23:14 15,98 10:23:19 16,08 10:23:24 16,27 10:23:29 16,01 10:23:34 15,72 10:23:44 15,92 10:23:49 15,99 10:23:54 16,13 10:23:59 16,34 10:24:04 16,5 10:24:14 15,89 10:24:19 15,58	10:23:04 15,65 50   10:23:09 15,84 50   10:23:14 15,98 50   10:23:19 16,08 50   10:23:24 16,27 50   10:23:29 16,01 50   10:23:34 15,72 50   10:23:44 15,92 50   10:23:49 15,99 50   10:23:54 16,13 50   10:23:59 16,34 50   10:24:04 16,5 50   10:24:14 15,89 50   10:24:19 15,58 50	10:23:04 15,65 50 494761,8   10:23:09 15,84 50 494769,5   10:23:14 15,98 50 494771,2   10:23:19 16,08 50 494772,5   10:23:24 16,27 50 494773,6   10:23:29 16,01 50 494777,7   10:23:34 15,72 50 49480,5   10:23:44 15,92 50 494800,5   10:23:49 15,99 50 494802,2   10:23:54 16,13 50 494802,9   10:23:59 16,34 50 494803   10:24:04 16,5 50 494802,9   10:24:14 15,89 50 494814,5   10:24:19 15,58 50 494825,6	10:23:04 15,65 50 494761,8 4067003   10:23:09 15,84 50 494769,5 4067001   10:23:14 15,98 50 494771,2 4067001   10:23:19 16,08 50 494772,5 4067000   10:23:24 16,27 50 494773,6 4067000   10:23:29 16,01 50 494777,7 4066999   10:23:34 15,72 50 494787,5 4066997   10:23:44 15,92 50 494800,5 4066995   10:23:49 15,99 50 494802,2 4066995   10:23:54 16,13 50 494802,9 4066995   10:23:59 16,34 50 494803 4066995   10:24:04 16,5 50 494802,9 4066995   10:24:14 15,89 50 494814,5 4066993   10:24:19 15,58 50 494825,6 4066990

ISSN: 2229-7359 Vol. 11 No. 3,2025

https://theaspd.com/index.php

PT982	10:24:34	14,81	50	494850,3	4066985	14,12
PT983	10:24:39	14,57	50	494858	4066984	14,06
PT984	10:24:44	14,54	50	494865,3	4066981	13,86
PT985	10:25:04	14,01	50	494901	4066974	13,83
PT986	10:25:09	14,02	50	494913,2	4066971	13,82
PT987	10:25:14	13,76	50	494933,7	4066967	13,83
PT988	10:25:19	13,7	50	494947,9	4066965	13,84
PT989	10:25:24	13,9	50	494950,7	4066964	13,85
PT990	10:25:29	14,12	50	494949,8	4066966	13,84
PT991	10:25:39	14,12	50	494954,2	4066965	13,85
PT992	10:25:44	13,74	50	494972,1	4066961	13,89

Scatter plots in terms of land surface temperature (LST) to explain the mean air temperature in Algiers in a study of urban heat islands (UHIs) in Figure 3 showed a moderate linear relationship with the regression equation of y = .0.111x + 16.66 and R2 = 0.752 indicating 75.2% of the variation in LST can be explained by air temperature. In the study, it was observed that land surface temperature (LST) varied from 13.5 °C to 15.0 °C when using vehicular surface-mounted sensors and LST ranged from 13.7 °C to 16.5 °C with nearly 0.15 to 0.94 °C of temperature difference. The spread of points about the regression line also reveals micro-scale variations that are likely caused by local environmental conditions, sensor limitations, or vehicular-related biases that make UHI monitoring challenging.

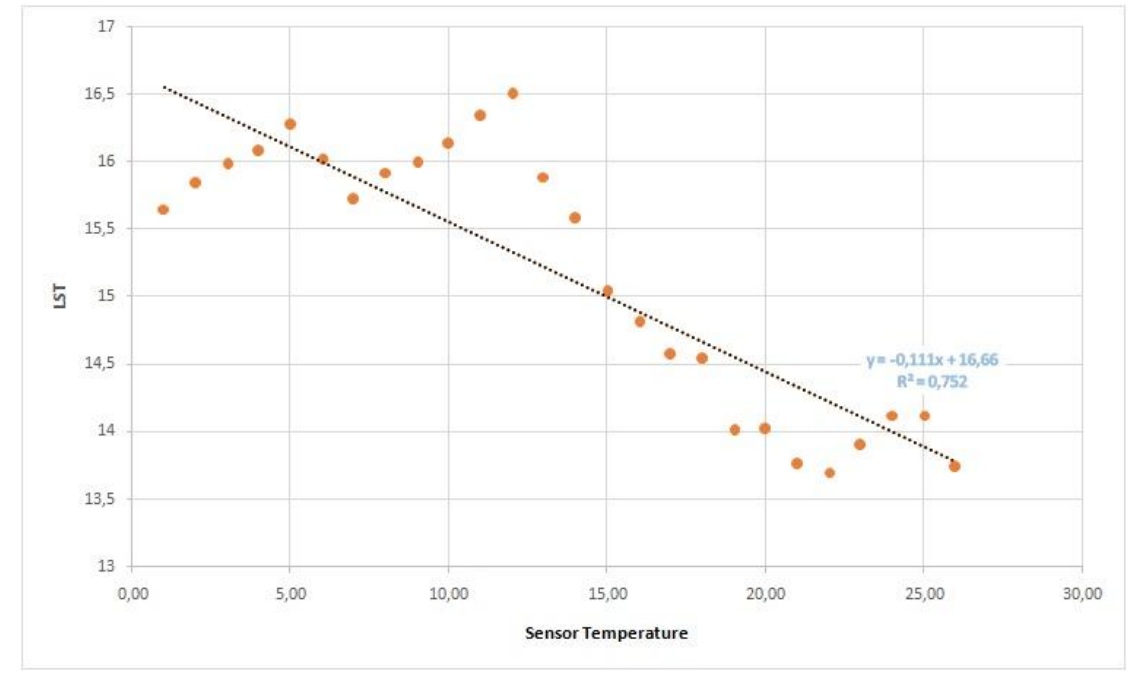


Figure 3. Relationship between land surface temperature (LST) and sensor temperature in Algiers region.

The spatial heterogeneity of the UHIs (urban heat islands) in Algiers is shown in Figure 4, which confirmed that there is a relationship between the land surface temperature (LST) with air temperature in this study (R<sup>2</sup> = 0.752). These differences we detect between red and blue zones exacerbate the difficulties in the measurement of UHIs, such as the inhomogeneities of mobile sensors, as well as the limitation of the temporal resolution by the Landsat 8 satellite around 11:30 (UTC +1) when the peak thermal time comes between 12:00 and 15:00 (Akbari et al., 2001). This figure (Fig. 4), which provides a visual baseline for the quantities that can be captured by the proposed smart monitoring approach, highlights areas of improvement, such as extending

sensor coverage and adding relative humidity data. As the conclusion mentions, it can be used, for instance, in the context of urban adaptation recommendations by introducing green belts, reflective materials, and such.



Figure 4. Interpolated TempSensor data on a Google Earth image background (Algiers, July 22nd, 2022).

The image 5 shows the interaction between vegetation cover and land surface temperatures, an important variable in the study of UHI in Algiers. The findings support the work of Yao et al., showing that regions that have low NDVI are primarily impermeable surfaces (impermeable surfaces (roads, buildings)) that underscore this UHI intensification. (2021) of the impact of impervious surface growth from 1990 to 2010. This map indicates that there is only a moderate correlation between LST and station air temperature (R<sup>2</sup> = 0.589), illustrating the general challenge of satellite data to capture thermal dynamics in real-time because of poor temporal resolution (one image every 16 days at 11:30) in combination with relatively sparse weather station's coverage. Here figure 5 demonstrates that the hybrid approach (mobile sensors + satellite data) is effective for micro-scale thermal detection.

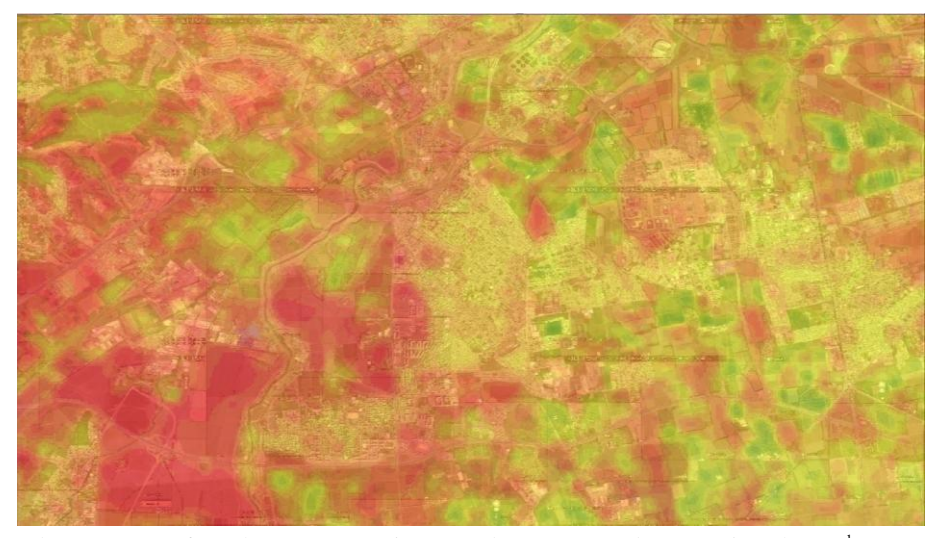


Figure 5. Landsat 8 image for Algiers region (LST and NDVI combination), July 23<sup>rd</sup>, 2022.

Figure 6 illustrates an interpolated temperature map overlaid on a QuickBird satellite image of the city of Algiers (Algiers Bay) with a colour gradient (similar to the previous figures in (Figure 4, Figure 5)) showing the distribution of UHI. The red and orange zones, which are in densely

ISSN: 2229-7359 Vol. 11 No. 3,2025

https://theaspd.com/index.php

urbanized areas near the port or urban clusters, indicate higher temperatures that are a consequence of dense buildings and impermeable surfaces. The blue zones, which are situated close to the coastline or a less urbanized area show lower temperatures likely due to the proximity of water and species composition empirical evidence of predisposed plant growth as moderate tree cover can be higher.



Figure 6. Interpolated TempSensor data on a Quick Bird image background (Algiers, July 23<sup>rd</sup>, 2022).

### **CONCLUSION**

So, by combining satellite data with a mobile temperature and humidity sensor, the present study has shown a successful hybrid approach for urban heat islands (UHIs) monitoring in Algiers in Algeria. This developed prototype outperforms conventional means using either fixed meteorological stations or Landsat imagery, allowing for higher temporal and spatial resolution to detect micro-scale temperature differences that would otherwise go unmeasured. Having an accuracy of R2 0.752 between mobile and satellite measurements, the results confirm the technology's potential to enhance the estimate of free-space temperature and to identify more accurately UHIs, even outside the satellite passing time, T11:30local time, when the phenomenon usually reaches its highest point, that is between T12:00 and T15:00. The practical consequences of this research are manifold. The first is the live upload of the data on a web server (www. heatislands. net) coupled with its visualization on Grafana offer a solid tool for decision makers to prevent and manage heat waves, which in a Mediterranean climate such as ours, is a raise of a great concern, especially at the peaks of July 2019 amazes heat peaks. This feature is consistent with Castro et al. (2024), highlighting the importance of real-time monitoring systems in helping cities respond to climate-related stressors. Second, the discovery of the previously unreported UHI regions highlights the opportunity for these types of findings to eventually be factored into urban planning strategies, via green belts or reflective materials, as previously noted by Amieur et al. (2022) in other areas of Algeria and validated by Aflaki et al. (2017) for their effectiveness in mitigation of urban temperatures. However, this leaves many opportunities for improvement. Extending mobile sensors would improve data coverage and representability, particularly in environmental niches like lakes, rooftops, and rugged terrain, where stationary sensors could be deployed (Shi et al., 2021). (2021) to improve thermal data collection. As highlighted by Li et al., a more in-depth assessment of relative humidity and its

ISSN: 2229-7359 Vol. 11 No. 3,2025

https://theaspd.com/index.php

relationship with temperature could enhance thermal models. (2020). The robustness of the results could also be enhanced by ongoing sensor calibration and cross-validation with other data sources (e.g. thermal drones), as successfully implemented recently by Henn et al. (2024) within densely built urban environments for studies of UHIs. In addition, Mohamed et al. (2024), this would provide the foundation to incorporate these data into predictive models that could give insights regarding the public health effects of UHIs, which are a major concern for climate-sensitive regions susceptible to extreme heat. Overall, this new form of solution, named for its smart monitoring characteristics, can provide a solid foundation for understanding UHIs in Algiers and managing their intensification. farms, showing the relevance of embedded technologies for the efforts of fostering countries' sustainable adaptation to climate change, and enabling similar applications at other cities with similar climatic and urban tendencies.

# Acknowledgement

We would like to express our gratitude to the *Office National de la Météorologie - ONM* (National Weather Center - Algiers, Algeria) for providing climatic ground data and important support.

#### Conflict of interest statement

On behalf of all authors, the corresponding author states that there is no conflict of interest.

### REFERENCES

- Akbari, H., Pomerantz, M., & Taha, H. (2001). Cool surfaces and shade trees to reduce energy use and improve air quality in urban areas. Solar Energy, 70(3), 295-310. https://doi.org/10.1016/S0038-092X(00)00089-X
- Mohamed, O. Y. A., & Zahidi, I. (2024). Artificial intelligence for predicting urban heat island effect and optimising land use/land cover for mitigation: Prospects and recent advancements. *Urban Climate*, 55, 101976. https://doi.org/10.1016/j.uclim.2024.101976
- 3. Arnfield, A. J. (2003). Two decades of urban climate research: A review of turbulence, exchanges of energy and water, and the urban heat island. *International Journal of Climatology*, 23(1), 1-26. https://doi.org/10.1002/joc.859
- Amieur, R., Rouag Saffidine, D., & Weber, C. (2022). Variations microclimatiques et effet de la végétation dans la ville aride de Ghardaïa, Algérie. VertigO la revue électronique en sciences de l'environnement, 22(3). https://doi.org/10.4000/vertigo.36719. Retrieved February 23, 2025, from http://journals.openedition.org/vertigo/36719
- Boukhabla, M., & Alkama, D. (2013). The effect of urban morphology on urban heat island in the city of Biskra in Algeria. International Journal of Ambient Energy, 34, 10.1080/01430750.2012.740424. https://doi.org/10.1080/01430750.2012.740424
- 6. Zhou, D., Xiao, J., Bonafoni, S., Berger, C., Deilami, K., Zhou, Y., Frolking, S., Yao, R., Qiao, Z., & Sobrino, J. A. (2019). Satellite Remote Sensing of Surface Urban Heat Islands: Progress, Challenges, and Perspectives. *Remote Sensing*, 11(1), 48. https://doi.org/10.3390/rs11010048
- 7. Ramírez Moreno, M. A., Keshtkar, S., Padilla Reyes, D., Ramos-López, E., García-Martínez, M., Hernández Luna, M., Mogro Zambrano, A., Mahlknecht, J., Huertas, J., Peimbert-García, R., Ramirez-Mendoza, R., Mangini, A., Pérez Henríquez, B., Roccotelli, M., & Lozoya-Santos, J. (2021). Sensors for sustainable smart cities: A review. *Applied Sciences*, 11(18), 8198. https://doi.org/10.3390/app11178198
- 8. Castro Medina, D., Guerrero Delgado, M., Sánchez Ramos, J., Palomo Amores, T., Romero Rodríguez, L., & Álvarez Domínguez, S. (2024). Empowering urban climate resilience and adaptation: Crowdsourcing weather citizen stations-enhanced temperature prediction. Sustainable Cities and Society, 101, 105208. https://doi.org/10.1016/j.scs.2024.105208
- 9. Heaviside, C., Macintyre, H., & Vardoulakis, S. (2017). The urban heat island: Implications for health in a changing environment. Current Environmental Health Reports, 4(3), 296-305. https://doi.org/10.1007/s40572-017-0150-3
- 10. Cao, S.-Y., Yin, W.-D., Su, J.-Y., Feng, C.-W., Du, Y.-C., Zhu, J.-Y., Ye, N., Ding, J.-Y., & Li, Y.-Z. (2023). Spatial and temporal evolution of multi-scale green space environments and urban heat islands: A case study of Beijing sub-center. Sensors and Materials, 35(2), 589-606. https://doi.org/10.18494/SAM4189
- 11. Shi, R., Hobbs, B. F., Zaitchik, B. F., Waugh, D. W., Scott, A. A., & Zhang, Y. (2021). Monitoring intra-urban temperature with dense sensor networks: Fixed or mobile? An empirical study in Baltimore, MD. *Urban Climate*, 39, 100979. https://doi.org/10.1016/j.uclim.2021.100979
- 12. Gémes, O., Tobak, Z., & Van Leeuwen, B. (2016). Satellite based analysis of surface urban heat island intensity. *Journal of Environmental Geography*, 9, 1-10. https://doi.org/10.1515/jengeo-2016-0004
- 13. Jiménez-Muñoz, J. C., Sobrino, J. A., Skoković, D., Mattar, C., & Cristóbal, J. (2014). Land surface temperature retrieval methods from Landsat-8 thermal infrared sensor data. *IEEE Geoscience and Remote Sensing Letters*, 11(10), 1840-1843. https://doi.org/10.1109/LGRS.2014.2312032

ISSN: 2229-7359 Vol. 11 No. 3,2025

https://theaspd.com/index.php

- 14. Li, X., Zhou, Y., Yu, S., Jia, G., Li, H., & Li, W. (2019). Urban heat island impacts on building energy consumption: A review of approaches and findings. *Energy*, 174, 407-419. https://doi.org/10.1016/j.energy.2019.02.183
- 15. Henn, K. A., & Peduzzi, A. (2024). Surface Heat Monitoring with High-Resolution UAV Thermal Imaging: Assessing Accuracy and Applications in Urban Environments. *Remote Sensing*, 16(5), 930. https://doi.org/10.3390/rs16050930
- 16. Şahin, M., Yıldız, B., Şenkal, O., & Peştemalci, V. (2011). Modelling and remote sensing of land surface temperature in Turkey. *Journal of the Indian Society of Remote Sensing*, 40, 1-10. https://doi.org/10.1007/s12524-011-0158-3
- 17. Masselot, P., Mistry, M., Vanoli, J., Schneider, R., Iungman, T., García-León, D., Ciscar, J.-C., Feyen, L., Orru, H., Urban, A., Breitner, S., Huber, V., Schneider, A., Samoli, E., de'Donato, F., Rao, S., Armstrong, B., Nieuwenhuijsen, M., & Aunan, K. (2023). Excess mortality attributed to heat and cold: A health impact assessment study in 854 cities in Europe. *The Lancet Planetary Health*, 7, e155-e164. https://doi.org/10.1016/S2542-5196(23)00023-2
- 18. Oke, T. R. (2002). Boundary layer climates. Routledge.
- 19. Office National des Statistiques. (2008). Recensement général de la population et de l'habitat 2008. https://www.ons.dz
- 20. Office National de la Météorologie. (2019). Rapport climatologique mensuel : Juillet 2019.
- 21. Chotchaiwong, P., & Wijitkosum, S. (2019). Relationship between land surface temperature and land use in Nakhon Ratchasima City, Thailand. Engineering Journal, 23(4), 1-12. https://doi.org/10.4186/ej.2019.23.4.1
- 22. Peng, S., Piao, S., Ciais, P., Friedlingstein, P., Ottle, C., Bréon, F.-M., & Myneni, R. B. (2012). Surface urban heat island across 419 global big cities. *Environmental Science & Technology*, 46(2), 696-703. https://doi.org/10.1021/es2030438
- 23. Aflaki, A., Mirnezhad, M., A., Ghaffarianhoseini, A., Omrany, H., Wang, Z.-H., & Akbari, H. (2017). Urban heat island mitigation strategies: A state-of-the-art review on Kuala Lumpur, Singapore, and Hong Kong. Cities, 62, 131-145. https://doi.org/10.1016/j.cities.2016.09.003
- Santamouris, M. (2015). Analyzing the heat island magnitude and characteristics in one hundred Asian and Australian cities and regions. Science of The Total Environment, 512-513, 582-598. https://doi.org/10.1016/j.scitotenv.2015.01.060
- 25. Marando, F., Heris, M., Zulian, G., Udias, A., Mentaschi, L., Chrysoulakis, N., Parastatidis, D., & Maes, J. (2021). Urban heat island mitigation by green infrastructure in European Functional Urban Areas. Sustainable Cities and Society, 77, 103564. https://doi.org/10.1016/j.scs.2021.103564
- 26. Sobrino, J. A., Jiménez-Muñoz, J. C., & Paolini, L. (2004). Land surface temperature retrieval from Landsat TM 5. Remote Sensing of Environment, 90(4), 434-440. https://doi.org/10.1016/j.rse.2004.02.003
- Stewart, I. D., & Oke, T. R. (2012). Local climate zones for urban temperature studies. Bulletin of the American Meteorological Society, 93(12), 1879-1900. https://doi.org/10.1175/BAMS-D-11-00019.1
- 28. Yao, R., Wang, L., Huang, X., Liu, Y., Niu, Z., Wang, S., & Wang, L. (2021). Long-term trends of surface and canopy layer urban heat island intensity in 272 cities in the mainland of China. Science of The Total Environment, 772, 145607. https://doi.org/10.1016/j.scitotenv.2021.145607
- 29. Tzyrkalli, A., Economou, T., Lazoglou, G., Constantinidou, K., Hadjinicolaou, P., & Lelieveld, J. (2024). Urban heat island trends in the Middle East and North Africa: A statistical approach. *International Journal of Climatology*. https://doi.org/10.1002/joc.8563
- 30. Voogt, J. A., & Oke, T. R. (2003). Thermal remote sensing of urban climates. Remote Sensing of Environment, 86(3), 370-384. https://doi.org/10.1016/S0034.4257(03)00079-8
- 31. Weng, Q., Lu, D., & Schubring, J. (2004). Estimation of land surface temperature-vegetation abundance relationship for urban heat island studies. Remote Sensing of Environment, 89(4), 467-483. https://doi.org/10.1016/j.rse.2003.11.005
- 32. Xian, G. Z. (2023). Characterizing urban heat islands across 50 major cities in the United States. U.S. Geological Survey Fact Sheet 2023–3048. https://doi.org/10.3133/fs20233048
- 33. Zhao, L., Lee, X., Smith, R. B., & Oleson, K. (2014). Strong contributions of local background climate to urban heat islands. *Nature*, 511(7508), 216-219. https://doi.org/10.1038/nature13462
- 34. Wang, W., Liu, K., Tang, R., & Wang, S. (2019). Remote sensing image-based analysis of the urban heat island effect in Shenzhen, China. *Physics and Chemistry of the Earth, Parts A/B/C, 110, 168-175.* https://doi.org/10.1016/j.pce.2019.01.002